Parasitology Open

cambridge.org/pao

Prolyl oligopeptidase-like deficient *Trypanosoma evansi* parasites are associated with reduced interleukin-10 concentrations *in vivo* and *in vitro*

Richard T. Kangethe[1], Eva M. Winger[1], Tirumala B.K. Settypalli[1], Viskam Wijewardana[1], Johanna Slaets[2], Theresa H. T. Coetzer[3] and Adama Diallo[1]*

[1]Animal Production and Health Laboratory, FAO/IAEA Agriculture and & Biotechnology Laboratory, IAEA Laboratories Seibersdorf, International Atomic Energy Agency (IAEA), Wagramer Strasse 5, P.O. Box 100, Vienna A1400, Austria; [2]Soil and Water Management & Crop Nutrition Laboratory, FAO/IAEA Agriculture and & Biotechnology Laboratory, IAEA Laboratories Seibersdorf, International Atomic Energy Agency (IAEA), Wagramer Strasse 5, P.O. Box 100, Vienna A1400, Austria and [3]Biochemistry, School of Life Sciences, University of KwaZulu-Natal (Pietermaritzburg campus), Private Bag X01, Scottsville 3209, South Africa

Abstract

The protozoan parasite *Trypanosoma evansi* is responsible for causing Surra in a variety of mammalian hosts over a wide geographical area. In the absence of an effective vaccine and increasing resistance to current chemotherapeutic agents, peptidases from the S9 prolyl oligopeptidase family have been identified as potential drug and vaccine targets. In order to understand the function of these peptidases during infection, three null mutant clones for prolyl oligopeptidase (*Δpop*), prolyl oligopeptidase-like (*Δpop-like*) and oligopeptidase B (*Δopb*) were generated in *T. evansi* RoTat 1.2 parasites and used for infection of mice. Mice inoculated with *T. evansi Δpop-like* mutants were able to survive longer than other groups of mice inoculated with *Δpop*, *Δopb* mutants or wild-type parasites. The regression analysis of plasma from mice-infected over time using *Δpop-like* mutants showed stable levels of interleukin-10 (IL-10) (non-significant slope, $P = 0{\cdot}171$) and declining IL-1b levels (negative slope, $P = 0{\cdot}04$) when compared with the wild-type control that demonstrated increasing levels of IL-10 and IL-1b ($P < 0{\cdot}01$ for both). Further analysis using mouse spleen cells in an *in vitro* 24 h incubation assay revealed that the percentage of IL-10 producing CD3 positive cells display significantly lower values when incubated with *Δpop-like* parasites than the wild-type clone ($P = 0{\cdot}002$). These results suggest that prolyl oligopeptidase-like peptidase may play a role in immune responses during *T. evansi* infections by affecting interleukin concentrations in the host.

Introduction

The mechanically transmitted protozoan parasite *Trypanosoma evansi*, a causative agent of the disease called Surra, is geographically the most widely distributed member of the genus *Trypanosoma* and infects the widest range of mammalian hosts, including buffaloes, camels, cattle, pigs, dogs, horses and goats (Holland *et al.* 2003; Dargantes *et al.* 2009; Desquesnes *et al.* 2013; Salah *et al.* 2015). *Trypanosoma evansi* parasites are transmitted by bloodsucking flies (*Tabanus* and *Stomoxys* spp.) (Hoare, 1972; Sumba *et al.* 1998) and also by vampire bats in South America (Hoare, 1965). Unlike *T. congolense*, a haemoparasite that is strictly restricted to the host blood vessels, the absence of *T. evansi* in the bloodstream can still result in pathogenic symptoms from parasites that have invaded host tissue (Holland *et al.* 2003; Desquesnes *et al.* 2013). The symptoms associated with *T. evansi* infections differ depending on the susceptibility of the infected host and include anaemia, fever, loss of weight and productivity as well as abortion (Vickerman *et al.* 1993; Desquesnes *et al.* 2013). In classical trypanosome infections, most of the symptoms emerge when the host immune system targets infective parasites. Parasites that die as a result of the host immune response release biologically active products that have been associated with disease symptoms (Taylor and Authié, 2004; Antoine-Moussiaux *et al.* 2009). These toxins include enzymes such as trypanosome peptidases that hydrolyse host proteins, trypanosome phospholipases that hydrolyse red blood cell membranes and trypanosome trans-sialidases that act as important factors for virulence and anaemia (Tizard *et al.* 1978; Antoine-Moussiaux *et al.* 2009; Coustou *et al.* 2012; Habila *et al.* 2012). The study of these factors, and in particular peptidases, led to the idea of developing new anti-disease vaccines that target trypanosome products that are associated with disease symptoms (Authié, 1994; Authié *et al.* 2001; Antoine-Moussiaux *et al.* 2009).

Several peptidases in *T. brucei*, *T. cruzi* and *Leishmania* spp. that belong to the S9 prolyl oligopeptidase family of clan SC serine proteases have been identified as potential drug and vaccine targets due to their unique properties (Coetzer *et al.* 2008; Bastos *et al.* 2013). Members of this family of serine peptidases in *T. brucei* (*Tbb*POP) and *T. cruzi* (*Tcr*POP) hydrolyse peptides smaller than 3 kDa at the carboxyl end of proline and alanine residues

Research Article

*Current address: Biological Systems Department – CIRAD, Control of Exotic and Emerging Animal Diseases (UMR15), TA A-15/G, Campus Int. Baillarguet, 34398 Montpellier Cedex 5, France.

Cite this article: Kangethe RT, Winger EM, Settypalli TBK, Wijewardana V, Slaets J, Coetzer THT, Diallo A (2017). Prolyl oligopeptidase-like deficient *Trypanosoma evansi* parasites are associated with reduced interleukin-10 concentrations *in vivo* and *in vitro*. *Parasitology Open* **3**, e17, 1–12. https://doi.org/10.1017/pao.2017.20

Received: 26 May 2017
Revised: 30 October 2017
Accepted: 31 October 2017

Key words:
Trypanosoma evansi; prolyl oligopeptidase-like; *Δpop-like* null mutants; IL-10; IL-1b

Author for correspondence:
Richard T. Kangethe, E-mail: R.T.Kangethe@iaea.org

CAMBRIDGE UNIVERSITY PRESS

(Bastos *et al.* 2005, 2010; Rawlings *et al.* 2016). Due to their catalytic properties, trypanosomal prolyl oligopeptidases have been implicated in the hydrolysis of host peptide hormones (Bastos *et al.* 2010). In *T. cruzi* infections, studies using inhibitors specific for *Tcr*POP prevented the parasite from infecting mammalian host cells (Bastos *et al.* 2005). Unlike other prolyl oligopeptidases, recombinantly expressed *Tcr*POP and *Tbb*POP are also capable of hydrolysing large substrates such as fibronectin and native collagen (Bastos *et al.* 2005, 2010). During *T. evansi* and *T. brucei* infections, oligopeptidase B, a serine peptidase with a preference for hydrolysing short peptides that contain di-basic residues, is released into the host bloodstream as an active peptidase that is not inhibited by host serpins where it has been implicated in hydrolysing host peptide hormones (Morty *et al.* 2001; 2005; Coetzer *et al.* 2008). The abnormal degradation of host atrial natriuretic factor by oligopeptidase B during *T. evansi* infection in rats is associated with increased blood volume, a situation that results in various disease lesions such as cardiomyopathy and heart failure (Morty *et al.* 2005). Oligopeptidase B in *T. cruzi* is crucial during the invasion of non-phagocytic host cells by stimulating the recruitment and fusion of lysosomes at the site of entry (Burleigh *et al.* 1997; Caler *et al.* 1998). In *Leishmania* spp., the deletion of oligopeptidase B leads to an accumulation of membrane associated enolase, an enzyme that has been implicated as a virulence factor (Swenerton *et al.* 2011). The activity of *Tbb*POP and other closely related *Tbb*POP-like peptidases has been shown to be dependent on the presence of *Tbb*OPB, where deletion of the gene for the latter leads to an increase in activity of POP-like peptidases (Kangethe *et al.* 2012). The interdependent role that both peptidases play in host peptide hormone hydrolysis is implied when looking at the amino acid residues present in mammalian peptide hormones, with many containing prolyl and alanyl, or arginyl and leucyl moieties (Kangethe *et al.* 2012).

To fully understand the role that serine oligopeptidases play in parasite physiology and host pathogenesis, prolyl oligopeptidase, prolyl oligopeptidase-like and oligopeptidase B null mutants (*Δpop*, *Δpop-like* and *Δopb*, respectively) were generated in *T. evansi* RoTat 1.2 parasites. Our results suggest that prolyl oligopeptidase-like serine peptidase is likely to influence host immune responses during infection by affecting interleukin concentrations in the host. These results would require further experiments using the bovine host in order to elucidate the mechanism of immune escape by *T. evansi* during infection.

Methods

Trypanosome culture

Bloodstream forms of *T. evansi* RoTat 1.2 wild-type were obtained from the Institute of Tropical Medicine, Antwerp, Belgium and were isolated in 1982 from a buffalo in Indonesia (ITMAS #020298) (Claes *et al.* 2002). Both bloodstream form wild-type parasites and null mutant clones generated were cultured in supplemented Iscove's Modified Dulbecco's Medium (IMDM) as previously described (Hirumi and Hirumi, 1989). Briefly, 1 L of IMDM containing 3·6 mM $NaHCO_3$ (Thermo Fischer Scientific, Roskilde, Denmark) was supplemented with 1 mM hypoxanthine, 1 mM sodium pyruvate, 0·16 mM thymidine, 0·05 mM bathocuprone sulphate, 1·0 mM L-cysteine and 0·2 mM 2-mercaptoethanol. The pH was adjusted to between 7·2 and 7·4 and 10% (v/v) heat-inactivated fetal calf serum (Gibco, Paisley, UK) was added before filtration using a 0·2 μm filter.

Generation of serine peptidase null mutants

Cloning

Trypanosoma evansi RoTat 1.2 strain genomic DNA was extracted from *in vitro* cultures as previously described (Medina-Acosta and Cross, 1993) and used as a template for PCR. The sequences flanking the POP, POP-like and OPB genes in *T. evansi* were identified in the Tritryp database (http://tritrypdb.org/tritrypdb/TevansiSTIB805) and primers designed as shown in Supplementary Table S1 with the respective expected sizes of amplification products indicated and restriction sites underlined.

The six generated PCR products were cloned into the TOPO® TA cloning vector (Thermo Fischer Scientific, Roskilde, Denmark) and serially sub cloned into two knock-out vectors bearing resistance for neomycin (pGLneo) (ten Asbroek *et al.* 1990) and blasticidin (pGLbla) (Kimura *et al.* 1994) to give pGLneo*Te*POP, pGLneo *Te*POP-like pGLneo*Te*OPB, pGLbla*Te*POP, pGLbla*Te*POP-like and pGLbla*Te*OPB, where the antibiotic resistance gene was flanked by the 5′ and 3′ regions of all three genes in both knock-out vectors. Orientation of the cloned 5′ and 3′ inserts was confirmed by PCR using vector and insert specific primers.

Parameters for transfection using the 4D-Nucleofector™ system

In order to transfect *T. evansi* RoTat 1.2 parasites, it was necessary to define the conditions required for the successful integration of recombinant plasmids in trypanosomes when using the 4D-Nucleofector™ system (Lonza, Levallois-Perret, France). Following recommendations from the manufacturer, an optimization experiment that combines 23 different Nucleofector™ programs with 5 different solutions (P1–P5) for a total of 115 reactions was set up.

(http://bio.lonza.com/fileadmin/groups/marketing/Downloads/Protocols/Generated/Optimized_Protocol_322.pdf)

Briefly, for each reaction, a pellet of 10^6 parasites was resuspended in 20 μL of solutions P1–P5 along with 1 μg of NotI-linearized pLEW20-green fluorescent protein (GFP), a plasmid that was previously used for GFP expression in *T. brucei* (Wirtz *et al.* 1999; Coustou *et al.* 2010), and transfected using one of the programs recommended by the manufacturer. Transfected parasites were first cultured for 24 h in the supplemented IMDM medium (Hirumi and Hirumi, 1989) before addition of 2 μg mL^{-1} of phleomycin for the selection of viable clones. Successful clones were analysed for GFP expression using flow cytometry. The successful combination of transfection program and P1–P5 solutions from the Nucleofector™ kit was established for gene knock-out experiments.

Transfection using serine peptidase knock-out plasmids

Briefly, a pellet of 10^7 parasites was resuspended in 100 μL of P solution and mixed with 10 μg of NotI-linearized pGLneo plasmid (pGLneo*Te*POP, pGLneo*Te*POP-like or pGLneo*Te*OPB) before transfection with the program setting identified as described above. Stably transfected trypanosomes were first cultured for 24 h before addition of neomycin (2·5 μg mL^{-1}). Single knock-out clones, generated by limiting dilution, were expanded and taken through a second round of transfection with the corresponding NotI-linearized recombinant pGLbla plasmid (pGLbla*Tev*POP, pGLbla*Tev*POP-like and pGLbla*Tev*OPB) and selected using both neomycin (2·5 μg mL^{-1}) and blasticidin (5 μg mL^{-1}) as described (Kangethe *et al.* 2012).

Confirmation of clones using Southern blot with digoxigenin-labelled probes and measurements of RNA abundance using the Affymetrix® whole transcript array

To confirm the stable transfection of both plasmids and the deletion of all three serine peptidase genes targeted in *T. evansi*, a Southern blot was carried out using digoxigenin probes according to the manufacturer's protocol (Roche, Mannheim, Germany). Briefly, two probes that spanned either the gene coding region (probe 1) or the external region of recombination

https://doi.org/10.1017/pao.2017.20

(probe 2) were prepared by PCR incorporating digoxigenin-labelled nucleotides. Enzyme-restricted genomic DNA isolated from the selected clones (PstI for *Tev*POP, SmaI for *Tev*POP-like and DraI for *Tev*OPB) was separated on a 1% (w/v) agarose gel (110 V for 4 h), transferred onto a DNA-binding nylon membrane (GE healthcare, Buckinghamshire, UK) using capillary action and cross-linked with UV before pre-hybridization at 42 °C and subsequent hybridization with each of the digoxigenin-labelled probes. Blots were washed with stringency buffer [0·3 M NaCl, 30 mM sodium citrate, pH 7·0 containing 0·1% (v/v) sodium dodecyl sulphate (SDS)] probed with anti-digoxigenin alkaline phosphatase (1:10 000) in Tris-buffered saline (0·1 M Tris–HCl, 0·1 M NaCl, pH 9·5) and revealed using chemiluminescent alkaline phosphatase substrate (Roche, Mannheim, Germany).

In order to further characterize the gene-deleted clones developed, RNA extracted from six replicates each of all three serine peptidase knock-out and wild-type clones was used for hybridization onto a whole transcript array for *Trypanosome* spp. developed by Affymetrix (Santa Clara, California, USA). RNA extraction was carried out using an extraction kit based on acid guanidinium thiocyanate (Chomczynski and Sacchi, 1987). Briefly, extracted RNA was processed through several cycles of amplification which include the first-strand cDNA synthesis, second-strand cDNA synthesis, *in vitro* cRNA synthesis and final second-cycle single-strand cDNA synthesis; all according to the manufacturer's protocol. Single-strand cDNA generated was fragmented, labelled and hybridized to the *Trypanosome* spp. whole transcript array before processing using the Gene Titan® Multi-Channel (MC) Instrument (Santa Clara, California, USA). Results generated where analysed using Affymetrix® Expression console software and interpreted with Affymetrix® Transcriptome Analysis Console (TAC) Software. Lists of genes were prepared using the *T. brucei* annotation with figures on fold change, analysis of variance (ANOVA) *P*-value and FDR (false discovery rate) adjusted *P*-value assigned to each gene described.

Enzymatic activity analysis of T. evansi *serine peptidase knock-out clones*

Parasites (1×10^7), were removed from culture, washed twice in phosphate-buffered saline (PBS), pH 7·2 and resuspended in 900 μL of 0·1% (w/v) Brij-35 in distilled water containing 10 μg mL^{-1} soyabean trypsin inhibitor (SBTI) to inhibit other parasite serine proteases, 10 μM L-trans-epoxysuccinyl-L-leucylamido(4-guanidino)butane (E-64) and 1 mM ethylenediaminetetraacetic acid (EDTA). The lysate was incubated for 10 min on ice, 100 μL of 10 × PBS added and centrifuged (10 000 ***g***, 5 min, 4 °C). The protein concentration of the lysate supernatant was determined using the bicinchoninic acid (BCA™) protein assay (Thermo Fischer Scientific, Massachusetts, USA). The hydrolysis of carboxybenzyl (Z)–Arg–Arg–7-amino-4-methylcoumarin (AMC), Z–Gly–Pro–AMC and Suc–Gly–Pro–Leu–Gly–Pro–AMC (Bachem, Torrance, USA) by the total parasite protein extract (5 μg) was determined for each clone. Briefly, parasite protein extract diluted in 0·1% (w/v) Brij-35 was incubated with assay buffer [200 mM Tris–HCl buffer, pH 8, 10 mM dithiothreitol (DTT) and 0·02% (w/v) NaN_3] for 10 min at 37 °C. Samples of the diluted parasite protein extract were combined with the appropriate fluorescent substrate (20 μM) and the fluorescence read (excitation at 360 nm and emission at 460 nm) using a Synergy H1 microplate reader (BioTek, Vermont, USA). Lysis buffer [0·1% (w/v) Brij-35, containing 10 μM E-64, 10 μg mL^{-1} SBTI, 1 mM EDTA and 1 × PBS] was used as a negative control. Parallel activity assays with inhibitors were carried out using 1 mM 4-(2-aminoethyl)benzenesulfonyl fluoride hydrochloride (AEBSF) for *Tev*OPB and 100 μM tosyl phenylalanyl chloromethyl ketone (TPCK) for *Tev*POP. When determining cysteine peptidase levels in total parasite extract, hydrolysis of Z–Phe–Arg–AMC was measured using the same protocol but with 10 μM E-64 replaced by 1 mM AEBSF and 1 μg ml^{-1} of pepstatin A. A parallel activity assay using 10 μM E-64 as an inhibitor for cysteine peptidases was performed. For statistical analyses, values were expressed as means ± standard error of the mean (S.E.M.). Significance tests were calculated by using two-way ANOVA and were considered significant at a P value < 0·05.

Mouse infections

In order to observe what role the three serine peptidases, *Tev*POP, *Tev*POP-like and *Tev*OPB play in *T. evansi* virulence and infection, one group of eight female, 8-week-old BALB/c mice for each gene deletion (three experimental groups housed together for each group) was inoculated by intraperitoneal injection using an insulin syringe with 1×10^4 *Δpop*, *Δpop-like* or *Δopb* *T. evansi* parasites per mouse resuspended in 50 μL of PBS. A control group was also infected with 1×10^4 *T. evansi* RoTat 1·2 wild-type parasites resuspended in 50 μL of PBS. Parasitaemia was measured on alternative days by bleeding from the tail and survival of mice was monitored during infection. Parasitaemia was estimated in each infected mouse using the rapid matching method as previously described (Herbert and Lumsden, 1976). Blood samples measured for parasitaemia were blinded to the readers. Plasma samples were also collected from the different groups of mice using heparinized capillary tubes over the course of infection and stored at −80 °C for further analysis. Mice were locally sourced and housed at the University of Veterinary Medicine in Vienna. Infection and care of infected mice was carried out using protocols approved by the institutional ethics committee of the University of Veterinary Medicine, Vienna and the national authority according to Section 26 of the Austrian Law for Animal Experiments, Tierversuchsgesetz 2012-TVG 2012 under the No. GZ 68·205/0069-WF/II/3b/2014.

Mouse Bio-Plex cytokine assay

A custom 10-plex Bio-Plex assay (Bio-Rad, Hercules, USA) was used to quantify the plasma levels of 10 interleukins in mouse (Mo) plasma [interferon-gamma (IFN-γ), tumour necrosis factor-alpha (TNF-α), IL-1α, IL-1β, IL-4, IL-6, IL-10, IL-12 (p40), IL12 (p70) and IL-13] as described by the manufacturer. Briefly, a 1 in 4 dilution of plasma collected at different time points from the different groups of mice was incubated with beads coupled to monoclonal antibodies specific for each component of the interleukin panel. Samples were washed before adding detection antibodies and developed for reading using the Bio-Plex® 200 suspension array system. Absolute interleukin concentrations were calculated using Bio-Plex Manager™ software.

Mouse spleen cell assay and intracellular IL-10 staining

Mouse spleen cells (10^6 per experiment) isolated from individual mice (3H-Biomedical, Uppsala, Sweden) were incubated with 5×10^5 parasites from *Tev*POP-like and *T. evansi* RoTat 1.2 wild-type clones in duplicate. Paired experiments were carried out for each vial of spleen cells to differentiate between different sources of mouse cells. Spleen cells were harvested 24 h after incubation and prepared for flow cytometry as previously described (Wijewardana *et al.* 2013). Briefly, cells were washed in PBS (pH 7·2) and resuspended in cell surface staining mix [fluorescence-activated cell sorting (FACS) buffer: PBS pH 7·2,

https://doi.org/10.1017/pao.2017.20

2% (v/v) foetal calf serum, anti-CD3 antibody-clone 145-2C11 and anti-CD8 antibody-clone 53-6·7; BD Biosciences, New Jersey, USA] and incubated for 30 min at 4 °C. Surface stained cells were washed in FACS buffer and stained using a live/dead staining mix containing an amine reactive dye (BD Biosciences) in FACS buffer for 15 min at 4 °C. The cells were then fixed and permeabilized using BD Cytofix/Cytoperm™ (BD Biosciences) according to the manufacturer's instructions. The fixed cells were resuspended in intracellular master mix (Permeabilization buffer, IL-10 antibody-clone JES5-16E3; BioLegend, San Diego, USA) and incubated for 30 min at 4 °C. The cells were given a final wash using permeabilization buffer and resuspended in FACS buffer. The stained cells were analysed using the Gallios™ flow cytometer (Beckman Coulter, California, USA) and results evaluated using Kaluza™ software (Beckman Coulter). The Wilcoxon matched-pairs rank test was used to calculate significance values.

Statistical analysis

In order to assess the effects of parasite gene deletion on host interleukins, a regression model was developed with plasma interleukin concentration as the quantitative response variable, parasitaemia and time after infection as quantitative predictors, and the gene deleted as a qualitative predictor variable. Two-way interactions between all predictor variables were included in the model. Because interleukin measurements were made from pooled plasma in each group of mice infected, two analytical replicates of the bulked sample of all mice within one treatment at each time point were obtained and the statistical analysis was then performed on these bulked values. Since parasitaemia values were obtained for each individual mouse, the parasitaemia values were averaged for mice within one treatment per time point. The detection limit for parasitaemia was 5×10^5 mL^{-1} when using the rapid matching method (Herbert and Lumsden, 1976). Observations below this limit do not meet the missing-at-random assumption, and therefore leaving them out can introduce bias into the analysis. To avoid this bias, a plug-in value of half of the detection limit was used wherever parasitaemia was not detectable (Barr *et al.* 2006). Parasitaemia was measured daily on the same mice for the duration of the study, and therefore bulked samples in time cannot be considered independent. This serial correlation was taken into account by fitting a linear mixed model with an additional random bulk-by-time effect, with the bulked samples as subject and a serial correlation structure in time for the random effect. Analytical replicates are independent between time points and therefore no serial correlation was modelled to the residuals. The structure of the variance–covariance matrix for the bulk-by-time effect was selected based on the Akaike information criterion (AIC) (Akaike, 1974). To this end, fixed effects and covariance structure were simultaneously estimated with the Restricted Maximum Likelihood algorithm (Patterson and Thompson, 1971). Tested were a first-order autoregressive and a compound symmetry structure. As the number of mice decreased over time, the variance of the random bulk-by-time effect was assumed to be inversely proportional to the number of mice samples in the bulk. This weighting allowed accounting for an increasing variance with a decreasing number of mice in a treatment over time. To implement the weighting using our mixed model software, we crossed the bulk-by-time effect with a continuous covariate that was equal to the inverse of the square root of the number of mice samples present in the bulk at the given time. This ensured that the variance of the random effect is inversely proportional to the number of mice samples in the bulk. Details on the weighting can be found in the Supplementary Section S2. Diagnostic plots were used to check the assumptions of normality and homoscedasticity. For the interleukin Mo IL-10 (mouse IL-10), a square root transformation was necessary to stabilize the variance. Input variable selection was then done with backward selection based on AIC, and for this purpose, models were fitted using Maximum Likelihood estimation. All analyses were performed with the MIXED procedure in SAS 9.4, and the serial correlation was accounted for using the RANDOM statement of the same procedure.

Results

Generation of T. evansi RoTat 1.2 serine peptidase null mutants

The conditions necessary for successful transfection of *T. evansi* RoTat 1.2 parasites using the 4D-Nucleofector™ system were established using the pLew20b-GFP plasmid. The matrix of 115 conditions recommended by the manufacturer yielded two combinations that produced viable clones: the program EF100 combined with solution P3 and the program DI100 with solution P5. Following the transfection, the potential recombinants were analysed for GFP fluorescence using flow cytometry (Supplementary Fig. S1). The combination of Program DI100 with solution P5 produced a higher number of clones when compared with program EF100 combined with solution P3 (results not shown) and was therefore chosen for future experiments.

The transfection of wild-type bloodstream forms of *T. evansi* RoTat 1.2 with pGLneo plasmids (pGLneo*Te*POP, pGLneo*Te*POP-like or pGLneo*Te*OPB) produced three distinct heterozygote clones resistant to neomycin; *Δpop*::NEO/POP, *Δpop-like*::NEO/POP-LIKE and *Δopb*::NEO/OPB. A second round of transfection with pGLbla plasmids (pGLbla*Te*POP, pGLbla*Te*POP-like or pGLbla*Te*OPB), using the respective single knock-out clones generated in the first round, resulted in the selection of three null mutant clones: *T. evansi* RoTat 1.2 *Δpop*, *T. evansi* RoTat 1.2 *Δpop-like* and *T. evansi* RoTat 1.2 *Δopb*, all of which were resistant to both blasticidin and neomycin. The deletion of *TevPOP*, *TevPOP-like* and *TevOPB* were confirmed by Southern blot using two probes for each deletion. Probe 1 was gene specific as shown for using *Tev*POP as an example, and probe 2 was an external probe that targeted a region outside the recombination region (Fig. 1A).

A Southern blot using the internal gene-specific probe 1 for *Tev*POP revealed a slightly >3000 bp fragment (see Fig. 1A for the expected sizes of the fragments) in PstI-restricted wild-type *T. evansi* RoTat 1.2 genomic DNA containing full length *Tev*POP (Fig. 1B, A1, L1). No band was detected when the same probe was used for PstI-restricted *Tev*Δpop null mutant genomic DNA (Fig. 1B, A1, L2). The external probe 2 also revealed a slightly >3000 bp fragment when incubated with PstI restricted wild-type RoTat 1.2 genomic DNA (Fig. 1B, A2, L1). To ensure that both resistance genes were in the right locus, a Southern blot using the external probe 2 on PstI-restricted *Tev*Δpop null mutant genomic DNA revealed a slightly >2000 bp fragment for NEO (Fig. 2B, A2, L2) and a slightly >1600 bp fragment for BLA (Fig. 1B, A2, L2). Southern blots were also carried out for *Tev*POP-like and *Tev*OPB null mutants using their respective probes. Probe 1 for *Tev*POP-like revealed a slightly >4000 bp band when using *T. evansi* RoTat 1.2 genomic DNA (Fig. 1B, B1, L1) with no band seen for *Δpop-like* (Fig. 1B, B1, L2). Probe 2 for *Te*POP-like also revealed a slightly >4000 bp band when using *T. evansi* RoTat 1.2 genomic DNA as expected (Fig. 1B, B2, L1), at slightly >1800 bp for NEO and slightly >1400 bp for BLA when using *Δpop-like* DNA (Fig. 1B, B2, L2). Probe 1 for *Tev*OPB revealed a slightly >2800 bp band when using *T. evansi* RoTat 1.2 genomic DNA (Fig. 1B, C1, L1) with no band seen for *Δopb* (Fig. 1B, C1, L2). Probe 2 for *Tev*OPB also revealed a slightly >2800 bp band when using *T. evansi* RoTat 1.2 genomic DNA

https://doi.org/10.1017/pao.2017.20

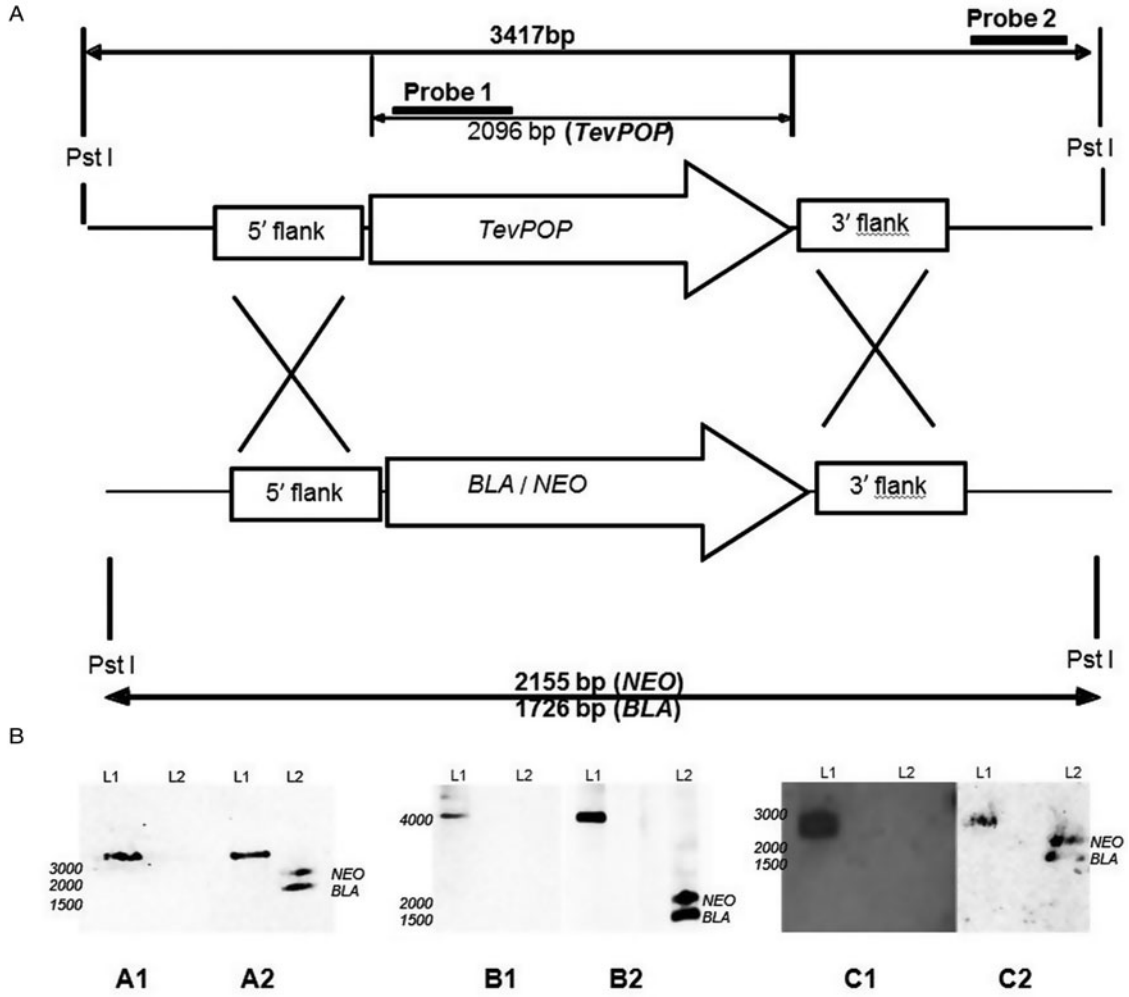

Fig. 1. Deletion of the *POP, POP-like* and *OPB* genes in *T. evansi* strain RoTat 1.2. (A) Schematic diagram showing the *TevPOP* locus. *TevPOP*, blasticidin (*BLA*) and neomycin (*NEO*) genes are shown by ⇨, 5′ and 3′ flanking regions by ▭. Probes prepared and the sizes expected on a Southern blot after restriction with PstI are in bold. *TevPOP* is used as a template with SmaI restriction for *TevPOP-like* and DraI restriction for *TevOPB*. (B) Southern blot of *T. evansi* RoTat 1.2 wild-type *TevΔpop*, *TevΔpop-like* and *TevΔopb* null mutants, *NEO* (neomycin);*BLA* (blasticidin). Numbers to the left indicate running positions of molecular mass markers. (A1) *T. evansi* RoTat 1.2 wild-type (L1) and *Δpop* null mutant (L2) genomic DNA incubated with probe 1 at slightly >3000 bp for *Tev*POP; (A2) incubated with probe 2 at slightly >3000 bp for *Tev*POP (L1), and at slightly >2100 bp and slightly >1700 bp for *NEO* and *BLA* respectively (L2). (B1) *T. evansi* RoTat 1.2 wild-type (L1) and *Δpop-like* null mutant (L2) genomic DNA incubated with probe 1 at slightly >4100 bp for *Tev*POP-like; (B2) incubated with probe 2 at >4100 bp for *Tev*POP-like (L1) and at >1800 bp and slightly >1400 bp for *NEO* and *BLA*, respectively (L2). (C1) *T. evansi* RoTat 1.2 wild-type (L1) and *Δopb* null mutant (L2) genomic DNA incubated with probe 1 at slightly >2800 bp for *Tev*OPB; (C2) incubated with probe 2 at slightly >2800 bp for *Tev*OPB (L1) and at slightly >2100 bp and slightly >1600 bp for *NEO* and *BLA*, respectively (L2).

(Fig. 1B, C2, L1), and at slightly >2100 bp for NEO and 1675 bp for BLA when using *Δopb* DNA (Fig. 1B, C2, L2).

Gene knock-out clones along with wild-type controls were also analysed using the Affymetrix whole transcript array specific for *Trypanosome* spp. Each group of gene deletion replicate clones were analysed using the *T. evansi* RoTat 1.2 wild-type clone as a positive control and gene lists generated using *T. brucei* TREU927 annotation. The top threefold change targets detected were Tb927·11·12850 (oligopeptidase B), Tb927·5·4300 (prolyl oligopeptidase-like) and Tb927·10·8020 (prolyl endopeptidase) with fold changes of −146·61, −108·62 and −104·02, respectively (Supplementary Table S2). This confirms that the targeted genes were correctly deleted in the experiment. The downregulation or upregulation of other genes observed in the array such as Tb927·2·170 (leucine-rich repeat protein) and Tb927·10·10240 (procyclin-associated gene 1 protein) are associated with variant surface glycoprotein expression, which switches periodically during an infection and as expected show a different expression profile when compared with the parasite clone used for annotation.

The growth of parasites *in vitro* was also analysed with no significant differences in replication observed between the different gene knock-out clones when compared with the wild-type (Supplementary Fig. S3).

Activity assays using serine peptidase null mutant clones

Lysates of *T. evansi* RoTat 1.2 *Δpop*, *Δpop-like* and *Δopb* null mutants and wild-type parasites were tested for serine peptidase activity using four substrates; Z–Phe–Arg–AMC, Z–Arg–Arg–AMC, Z–Gly–Pro–AMC and Suc–Gly–Pro–Leu–Gly–Pro–AMC. Whereas Z–Arg–Arg–AMC is the preferred substrate for oligopeptidase B hydrolysis (Coetzer *et al.* 2008), Z–Gly–Pro–AMC and Suc–Gly–Pro–Leu–Gly–Pro–AMC are both used for measuring prolyl oligopeptidase activity with Suc–Gly–Pro–Leu–Gly–Pro–AMC appearing to be a better substrate than Z–Gly–Pro–AMC (Bastos *et al.* 2010).

All the mutant and wild-type parasites were able to hydrolyse Z–Phe–Arg–AMC, a substrate routinely used for measuring the activity of parasite cysteine peptidases and used as a control in this experiment (Mbawa *et al.* 1992; Caffrey *et al.* 2001). Wild-type *T. evansi* RoTat 1.2 parasites readily hydrolysed Z–Arg–Arg–AMC (expressed as 100% activity), while the *Δpop* and

https://doi.org/10.1017/pao.2017.20

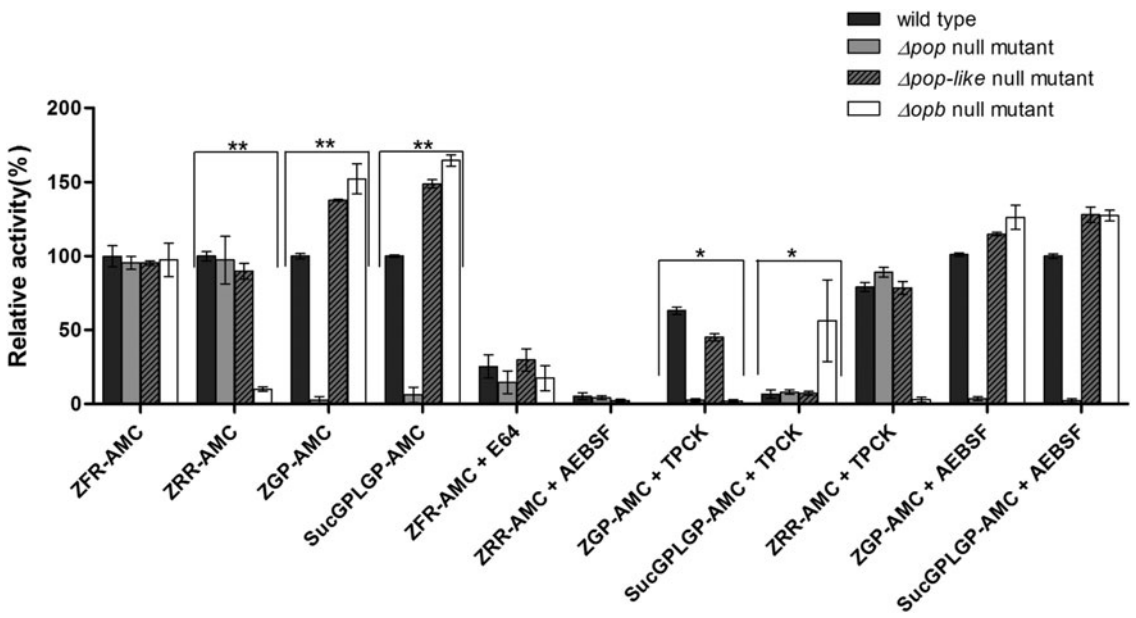

Fig. 2. Enzymatic characterization of null mutant parasites. The hydrolysis of OPB substrates, Z–Arg–Arg–AMC (ZRR–AMC) and Z–Phe–Arg–AMC (ZFR–AMC) and POP substrates Z–Gly–Pro–AMC (ZGP–AMC) and Suc–Gly–Pro–Leu–Gly–Pro–AMC (SucGPLGP–AMC) by lysates of *Δopb* null mutant, *Δpop* null mutant and *Δpop-like* null mutant and *T. evansi RoTat 1.2* wild-type parasites was assessed with or without specific inhibitors E64, AEBSF or TPCK included in the assay. Data are presented as means ± S.E.M. ($n = 3$) of fluorescence values plotted relative to the wild-type as a percentage for each experiment, with no lysate fluorescence deducted from each value as background. $^{**}P < 0{\cdot}001$ and $^{*}P < 0{\cdot}05$ were calculated in comparison to the wild-type.

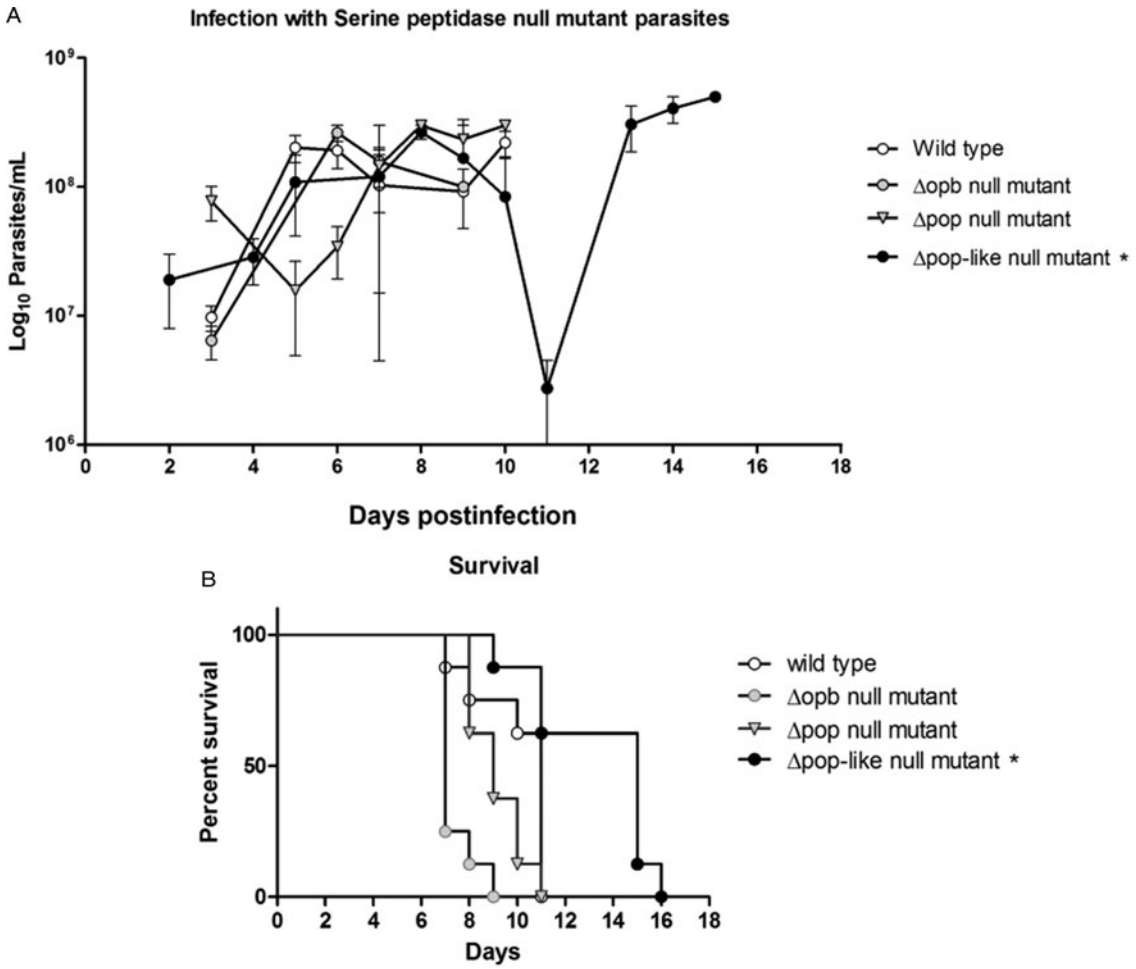

Fig. 3. Mice infected using *T. evansi Δpop-like* null mutants survive significantly longer when compared with groups infected with the wild-type parasites or other mutants generated in this study. (A) Parasitaemia in mice infected with *T. evansi RoTat 1.2* wild-type parasites compared with *Δopb* null mutant-, *Δpop* null mutant- and *Δpop-like* null mutant infected mice. Each value is a mean of 8 mice. Intraperitoneal infections were carried out using 1×10^4 parasites per mouse. (B) Kaplan–Meier survival analysis for mice infected with *T. evansi RoTat 1.2* wild-type parasites compared with *Δopb* null mutant, *Δpop* null mutant and *Δpop-like* null mutant ($n = 8$ in each group) $^{*}P < 0{\cdot}05$ in comparison to the wild-type.

https://doi.org/10.1017/pao.2017.20

Δpop-like null mutants displayed similar activities at equal and approximately 90% of that of the wild-type, respectively (Fig. 2). The *Δopb* null mutant parasites were unable to hydrolyse Z–Arg–Arg–AMC and gave comparable values to the no-lysate control as expected (Fig. 2). The substrates Z–Gly–Pro–AMC and Suc–Gly–Pro–Leu–Gly–Pro–AMC were used to characterize the *Δpop* null mutant clones and as expected were unable to hydrolyse either substrates (Bastos *et al.* 2005, 2010). Interestingly, *Δpop-like* mutant clones retained their ability to hydrolyse both Z–Gly–Pro–AMC and Suc–Gly–Pro–Leu–Gly–Pro–AMC substrates with a significantly higher activity (Fig. 2). A similar trend is seen with the *T. evansi Δopb* null mutant, a phenomenon that has previously been observed in oligopeptidase B null mutants when using Z–Gly–Pro–AMC as a substrate (Kangethe *et al.* 2012)

The effect of class specific inhibitors was also included in the activity assay in order to further characterize the activity of the mutant clones generated. The inhibitors E-64 and AEBSF effectively inhibited the hydrolysis of Z–Phe–Arg–AMC and Z–Arg–Arg–AMC respectively in all mutant and wild-type parasites (Fig. 2). The effect of TPCK on the hydrolysis of Z–Gly–Pro–AMC by wild-type and *Δpop-like* mutant parasites was incomplete when compared with *Δopb* null mutants (Fig. 2). This effect is however reversed when using Suc–Gly–Pro–Leu–Gly–Pro–AMC as a substrate where *Δopb* null mutants retain activity in the presence of TPCK when compared with wild-type and *Δpop-like* mutant parasites (Fig. 2). When Z–Arg–Arg–AMC hydrolysis was performed with TPCK and Z–Gly–Pro–AMC or Suc–Gly–Pro–Leu–Gly–Pro–AMC with AEBSF, all mutant and wild-type parasites displayed profiles similar to when hydrolysis was carried out without inhibitors (Fig. 2).

Evaluation of the T. evansi *RoTat 1.2* Δpop, Δpop-like *and* Δopb *null mutants in mice*

Mice were inoculated with the three different *T. evansi* mutants in parallel with wild-type parasites in order to observe their *in vivo* dynamics. *T. evansi* RoTat 1.2 wild-type infections in mice were significantly virulent with a pre-patent period of 2 days (Fig. 3A) and a median survival rate of 11 days (Fig. 3B). The group of mice infected with *T. evansi Δpop-like* null mutant parasites survived longer than mice infected with control *T. evansi* RoTat 1.2 wild-type parasites with a median survival rate of 15 days compared with 11 days in the control group (Fig. 3B). Mice infected with *T. evansi Δpop-like* null mutant parasites were also able to survive the first wave of parasitaemia when compared with the wild-type control, although the parasitaemia profiles in terms of numbers were similar to the wild-type control (Fig. 3A). The two groups of mice infected with either *T. evansi Δpop* or *T. evansi Δopb* null mutant parasites did not survive significantly longer than the control group with median survival rates of 9 and 7 days, respectively (Fig. 3B), and did not recover from the first wave of parasitaemia (Fig. 3A).

Comparison of interleukin levels in mice inoculated with T. evansi *RoTat 1.2* Δpop, Δpop-like, Δopb *and wild-type parasites*

Plasma collected from each group of infected mice over different days of infection was measured for ten different interleukin levels (Supplementary Fig. S2). For all interleukin concentrations, the effect of parasitaemia and its interaction terms was non-significant and therefore this variable was dropped from the models. Furthermore, non-significant changes in interleukin concentration over time were observed in mouse blood; with the exception of IL-10 and IL-1b (Fig. 4) where both time after infection, parasite clone and the interaction between these two variables were significant. The significant interaction term indicates that the interleukin concentration of IL-10 and IL-1b evolves differently over time for the various parasite types.

The plasma levels of IL-10 in *T. evansi* RoTat 1.2 wild-type infections increased significantly over time (slope estimate of

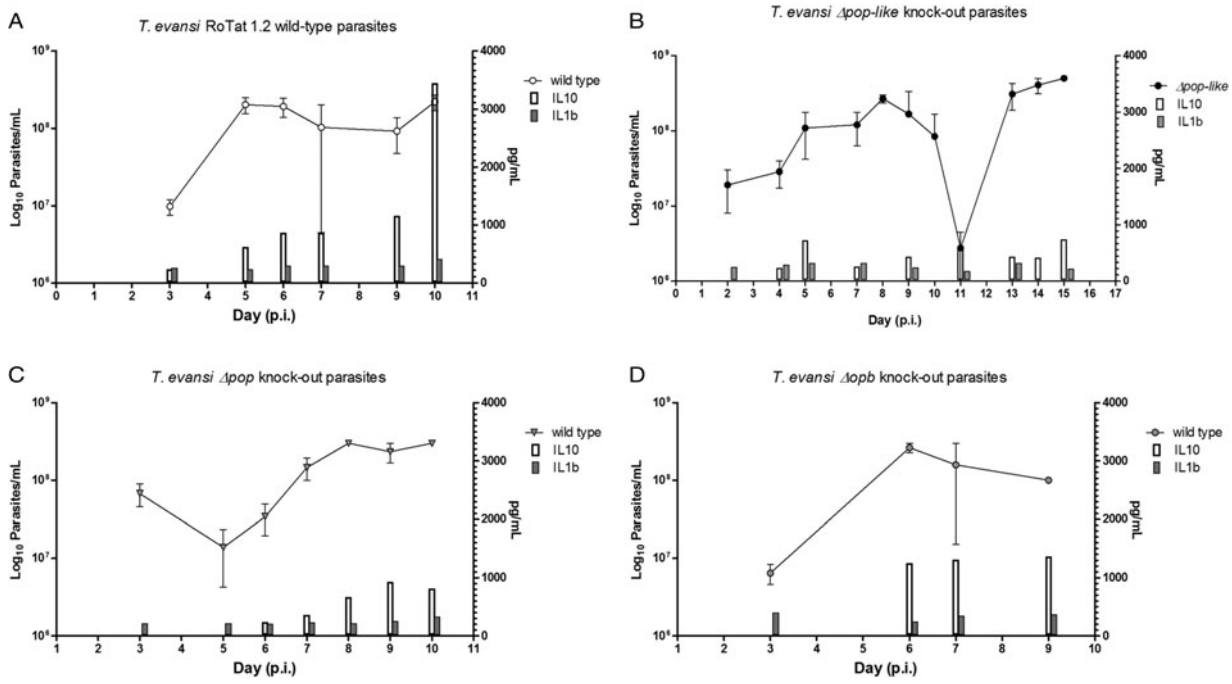

Fig. 4. Plasma analysis for IL-10 and IL-1b. (A) Plasma collected from a group of eight mice infected using *T. evansi* RoTat 1.2 wild-type parasites per mouse was measured for different interleukin concentrations including IL-10 and IL-1b that displayed a significant difference and plotted as pg mL^{-1} on the secondary *Y*-axis; (B) Interleukin measurements in plasma collected from mice infected with *Δpop-like* null mutant parasites; (C) Interleukin measurements in plasma collected from mice infected with *Δpop* null mutant parasites; (D) Interleukin measurements in plasma collected from mice infected with *Δopb* null mutant parasites. Intraperitoneal infections were carried out using 1×10^4 parasites per mouse. The lower limits of detection using luminex were 61·524 pg mL^{-1} for IL-10 and 112·732 pg mL^{-1} for IL-1b. Any measurements that fell below these limits were plotted as 0 in the graphs above.

https://doi.org/10.1017/pao.2017.20

Table 1. Parameter estimates for the fixed effects of the linear mixed model for Interleukin IL-10 concentration in mice infected with gene deleted parasites, obtained with Restricted Maximum Likelihood and a random bulk-by-time effect weighted for the decreasing number of surviving mice, and significance tests for the slope estimates for the interaction term time after infection and parasite type *$P < 0{\cdot}05$, **$P < 0{\cdot}001$

Regression equation for IL-10	Gene deleted	Estimate	Standard error	DF	*t*-value	$P > \|t\|$	Time trend
SQRT(Mo IL-10)=0+4·4387*days_post_analysis	*Δopb*	4·4387	1·0851	12·1	4·09	0·0015*	Increase
SQRT(Mo IL-10)=0+1·8588*days_post_analysis	*Δpop*	1·8588	0·4491	10·5	4·14	0·0018*	Increase
SQRT(Mo IL-10)=4·0969+0*days_post_analysis	*Δpop-like*	0·2995	0·2045	11	1·46	0·171	No change
SQRT(Mo IL-10)=−14·7836 +4·7985*days_post_analysis	wild-type	4·7985	0·585	13·4	8·2	<0·0001**	Strong increase

Table 2. Parameter estimates for the fixed effects of the linear mixed model for Interleukin IL-1b concentration in mice infected with gene deleted parasites, obtained with Restricted Maximum Likelihood and a random bulk-by-time effect weighted for the decreasing number of surviving mice and significance tests for the slope estimates for the interaction term time after infection and parasite type *$p < 0{\cdot}05$

Regression equation for IL-1b	Gene deleted	Estimate	Standard error	DF	*t*-value	$P > \|t\|$	Time trend
Mo IL-1b=0+4·7003*days_post_analysis	*Δopb*	4·7003	1·5247	14	3·08	0·0081*	Increase
Mo IL-1b=0+0*days_post_analysis	*Δpop*	1·5323	0·7821	14	1·96	0·0699	No change
Mo IL-1b=11·9251 + −1·0933*days_post_analysis	*Δpop-like*	−1·0933	0·5083	16	−2·15	0·0475*	Decrease
Mo IL-1b=0+3·401*days_post_analysis	wild-type	3·401	0·9996	17	3·4	0·0033*	Increase

4·8, $P < 0{\cdot}001$, Table 1) and were highest before the mice succumbed to disease (Fig. 4A). The plasma levels of IL-1b in mice inoculated with wild-type parasites also increased significantly as the infection progressed (slope estimate of 3·401, $P < 0{\cdot}05$, Table 2), although this was not as dramatic as the increase in IL-10 plasma concentrations.

A different scenario was observed in the group of mice infected using *T. evansi Δpop-like* null mutants, where the concentration of IL-10 in plasma did not change significantly as infection progressed (Fig. 4B). Statistical analysis confirmed this trend with a *P*-value of 0·171 (Table 1). Interestingly, however, IL-1b interleukin values dropped significantly as infection with *Δpop-like* null mutants progressed (slope estimate −1·09, Table 2, Fig. 4B), with a *P*-value of 0·04 whereas wild-type infections showed a significant positive slope (estimate 3·4, *P*-value <0·05, Table 2).

Infections using *Δpop* and *Δopb* null mutants followed a similar trend to infections using *T. evansi* wild-type parasites (Figs. 4C and D respectively). In both of these infections, IL-10 production increased along with IL-1b as disease progressed (Tables 1 and 2).

In vitro *analysis of IL-10 production in mouse spleen cells*

In order to confirm the effect of reduced IL-10 production in mice, naïve BALB/c mouse spleen cells were incubated in paired experiments using both *T evansi* wild-type and *TevΔpop-like* parasites. The characerization of the incubated spleen cells using flow cytometry revealed that $CD3^+$ T lymphocytes are responsible for the production of IL-10 in mouse spleens (Fig. 5A). A total of ten replicate experiments using different vials of mouse spleen cells in paired experiments consistently showed that *T. evansi* RoTat1.2 wild-type parasites elicited a higher percentage of T cells producing IL-10 when compared with experiments using *TevΔpop-like* parasites. Statistical analysis using the Wilcoxon matched-pairs signed rank test confirmed this trend giving a *P* value of 0·002 when ranking wild-type parasites with *TevΔpop-like* clones and a *P* value of 0·04 when compared with cells incubated without parasites (Fig. 5B).

Discussion

The role of parasite prolyl oligopeptidases (POPs) in host physiology is closely linked to the catalysis of mammalian peptides during infection (Bastos *et al.* 2005; 2010; 2013; Kaszuba *et al.* 2012; Fajtová *et al.* 2015). Although POPs from different species share similar three-dimensional structures, divergences have been observed between species in terms of inhibition and the specificity of substrates that they hydrolyse (Kaszuba *et al.* 2012; Bastos *et al.* 2013). Whereas recombinant POPs from *T. brucei* and *T. cruzi* are capable of hydrolysing proline rich native collagen, recombinant POP from *Schistosoma mansoni* is unable to hydrolyse substrates such as human collagens type I and IV (Bastos *et al.* 2005, 2010; Fajtová *et al.* 2015). The exact physiological functions of POPs are yet to be fully understood, with functions seemingly related to the infective species. These divergences in function are hinted at even within the same species, with a twofold increase in the expression of procyclic POP in *T. brucei* compared with bloodstream forms of the parasite (Bastos *et al.* 2010). In this study, we observed a possible role for a POP-like peptidase from *T. evansi* in terms of affecting the concentrations of interleukin 10 in plasma during infection in mice. A recent study that screened 20 serine peptidase genes using RNA interference, nine of which belong to the S9 family, described an essential role for a putative type-I signal peptide peptidase (Moss *et al.* 2015). Oligopeptidase B, putative POP and prolyl oligopeptidase-like from *T. b. brucei* (*Tbb*OPB, *Tbb*POP and *Tbb*POP-like; Gene IDs Tb927·11·12850, Tb927·10·8020 and Tb927·5·4300, respectively) were all included in the screen. A reduction of approximately between 75% for *Tbb*POP and 25% for *Tbb*POP-like did not display any phenotype both *in vitro* and during mouse infections. This was, however, not unexpected, as earlier RNAi experiments targeting *Tbb*POP with a knockdown efficiency of up to 80% showed no effect on parasite viability (Bastos *et al.* 2010). The deletion of *Tbb*OPB was also previously shown to have no effect on the viability or virulence of *T. brucei* 427 Lister parasites (Kangethe *et al.* 2012). The present study showed that the deletion of the *Tev*POP-like gene has a different effect on *T. evansi* parasites when used for mouse infections, with the group of mice infected able to survive the first wave of parasitaemia and with a longer median survival rate of 15 days

https://doi.org/10.1017/pao.2017.20

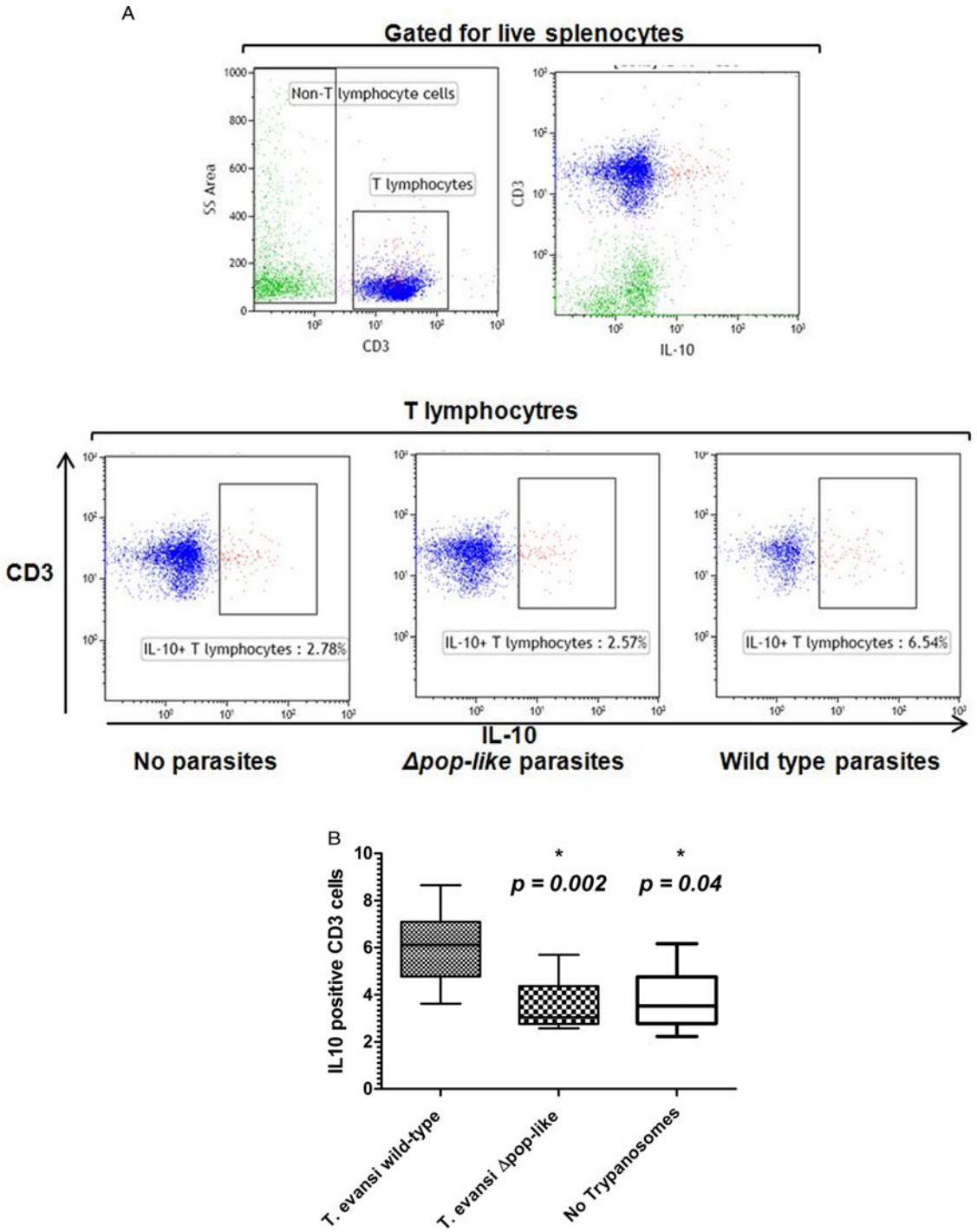

Fig. 5. Flow cytometry analysis of naïve mouse spleen cells (A) Representative flow cytometry plots illustrating the gating strategy used to define IL-10 producing $CD3^+$ T lymphocytes (blue) versus Non-T lymphocytes (green). (B) Wilcoxon matched-pairs signed rank test reveals a significant difference between cells incubated with wild-type parasites when compared with spleen cells incubated with *Δpop-like* clones at a *P* value of 0·002. Differences between spleen cells incubated with *Δpop-like* and non-incubated cells are not significant.

when compared with 11 days in the wild-type infection control. Interestingly, the generation of *Δopb* and *Δpop-like* null mutants in *T. evansi* parasites resulted in an increase in the hydrolysis of Z–Gly–Pro–AMC and Suc–Gly–Pro–Leu–Gly–Pro–AMC, both of which are substrates used to assay for recombinant *T. b. brucei* POP (Bastos *et al.* 2005). The increase in activity for Z–Gly–Pro–AMC when the gene for oligopeptidase B is deleted has been observed in *T.b. brucei Δopb* null mutants (Kangethe *et al.* 2012). When class specific inhibitors were used to assay the activity of the mutants generated in the present study, it was shown that *Δpop-like* parasites retained approximately half their activity when incubated with TPCK before the incubation with Z–Gly–Pro–AMC, similar to wild-type parasites. Interestingly, this activity is inhibited in *Δopb* parasites, which instead shows residual activity when using Suc–Gly–Pro–Leu–Gly–Pro–AMC as a substrate after incubation with TPCK. This would imply that the increase in POP activity seen when deleting *TevOPB* can be attributed to *Tev*POP, whereas deleting *TevPOP-like* affects the activity of another unknown peptidase with POP activity.

Plasma collected from mice over the course of infection with all three null mutants and the wild-type control was measured for ten different interleukin concentrations (Supplementary data Fig. S2). Statistical analysis of absolute interleukin concentrations in correlation with parasitaemia revealed that IL-10 levels in mice

https://doi.org/10.1017/pao.2017.20

infected using *T. evansi Δpop-like* mutants did not significantly change when compared with the wild-type control, whereas IL-1b levels gradually declined but with less significance when compared with wild-type controls. In order to further study the effect of deleting the *TevPOP-like* gene on IL-10 production, an *in vitro* assay using BALB/c mouse splenocytes showed that $CD3^+$ T-lymphocytes are the major producers of IL-10 and their ability to secrete IL-10 is reduced when incubated with *Δpop-like* parasites as opposed to the wild-type strain. During *Leishmania mexicana* infections in C57BL/6 mice, T cell-derived IL-10 was observed during the chronic phase of infection as opposed to classical immune suppression by IL-10 producing macrophages or dendritic cells (Bastos *et al.* 2013). These IL-10-producing T cells could be $CD4^+CD25^+$and $FoxP3^+$ regulatory T cells, which suggests that wild-type parasites induce immune suppression at the onset of the infection. When *Δpop-like* null mutants were incubated with mouse splenic cells *in vitro*, a reduction in IL10 expression suggests that POP-like protease may play a role in regulating the production of the interleukin in host cells. Future experiments are required to ascertain which sub-type of T cells produce regulatory IL-10 and further elucidate which role parasite POP-like protease plays in host IL-10 production. Other parasite peptidases that have also been shown to inhibit Th1 responses during infection include a cysteine protease B from *Leishmania mexicana* and cathepsin B from *Leishmania chagasi*, that cleave human TGF-β, a cytokine that regulates IL-10 and thereby affecting immunosuppression (Somanna *et al.* 2002; Buxbaum *et al.* 2003; Buxbaum, 2015).

In classical trypanosome infections, initial pro-inflammatory type I immune responses mediated by IFN-γ, nitric oxide (NO) and TNF are necessary for controlling the first wave of parasitaemia (Namangala *et al.* 2001b; Stijlemans *et al.* 2007; Baral, 2010). Interleukin 1b is also a strong mediator of inflammatory immune responses during *T. brucei* infections (Nyakundi *et al.* 2002). A sustained type I response is however deleterious to the mammalian host and type II non-inflammatory responses mediated by IL-4 and -10 are required later during infection to prevent immune mediated pathologies (Namangala *et al.* 2001a; Antoine-Moussiaux *et al.* 2008; Kato *et al.* 2015). In contrast, *T. evansi* infections in C57BL/6 mice do not require a type I inflammatory response in order to control parasitaemia with the role of IgM proven to be more crucial (Baral *et al.* 2007). TNF, TNF receptor gene, IFN-γ and Inducible nitric oxide synthase (iNOS) groups of knockout mice infected with *T. evansi* parasites all developed parasitaemia and survived at a similar rate as wild-type C57BL/6 mice suggesting that the main determinants for inflammatory response were not crucial for survival and parasitaemia in mice (Baral *et al.* 2007). When B-cell deficient and IgM deficient groups of mice were used for *T. evansi* infection studies, the loss of first peak parasitaemia control and subsequent rapid death was observed when compared with wild-type C57BL/6 mice. The passive transfer of IgM antibodies to B cell deficient mice restored parasite control indicating a significant contribution to protection (Baral *et al.* 2007).

The role of non-inflammatory IL-10 mediated responses during *T. evansi* infections has been studied in mice and cattle (Mekata *et al.* 2012, 2015). Mice infected with *T. evansi* strain L2 showed a strong up-regulation of IL-10 and CCL8 which were responsible for the expansion of regulatory dendritic cells (DCs) during the acute phase of parasite infection (Mekata *et al.* 2012). Inoculation of mice with regulatory DCs significantly prolonged their survival rate after infection when compared with untreated controls (Mekata *et al.* 2012). This indicated that regulatory DCs inhibited the production of pro-inflammatory cytokines associated with acute pathology during *T. evansi* infections in mice. The upregulated expression of CCL8 and IL-10 has also been detected in cattle experimentally infected with *T. evansi* parasites (Mekata *et al.* 2015).

Our model for infection shows that BALB/c mice infected with either *TevΔopb* or *TevΔpop* parasites does not change the course of infection when compared with infections initiated using *T. evansi* RoTat 1.2 wild-type parasites. *T. evansi Δpop-like* mutants are also able to infect mice in a similar manner to wild-type parasites although the mice infected are able to survive longer and are associated with a lower expression of IL-10 during infection. We do however need to stress that the altered interleukin levels observed in this study could be as a result of other factors other than the deletion of POP-like peptidase.

In conclusion, we were able to generate *T. evansi Δpop*, *Δpop-like* and *Δopb* null mutant parasites and show that mice infected using *T. evansi Δpop-like* parasites were able to survive longer when compared with wild-type infections and were associated with lower IL-10 production. The association observed between *Δpop-like* parasites and IL-10 was also observed using a splenocyte *in vitro* assay. It must be emphasized that in order to fully understand the role of POP-like peptidase during *T. evansi* infections, experiments need to be carried out in the natural host where a more natural chronic infection is possible. This is particularly important in order to further elucidate the role of POP-like peptidase during the course of parasite infection.

Supplementary material. The supplementary material for this article can be found at https://doi.org/10.1017/pao.2017.20

Acknowledgements. We thank Jeremy C. Mottram from the Wellcome Trust Centre for Molecular Parasitology at the University of Glasgow for providing the knock-out vectors and Philippe Büscher from the Institute of Tropical Medicine in Antwerp for providing the *T. evansi* Rotat 1.2 strain.

Financial Support. This work was supported by The African Renaissance Fund.

Conflicts of Interest. The authors have nothing to disclose.

References

Akaike H (1974) A new look at the statistical model identification. *IEEE Transactions on Automatic Control* **19**, 716–723.

Antoine-Moussiaux N, Magez S and Desmecht D (2008) Contributions of experimental mouse models to the understanding of African trypanosomiasis. *Trends Parasitology* **24**, 411–418.

Antoine-Moussiaux N, Buscher P and Desmecht D (2009) Host-parasite interactions in trypanosomiasis: on the way to an antidisease strategy. *Infection and Immunity* **77**, 1276–1284.

Authié E (1994) Trypanosomiasis and trypanotolerance in cattle: a role for congopain? *Parasitology Today* **10**, 360–364.

Authié E, Boulangé A, Muteti D, Lalmanach G, Gauthier F and Musoke AJ (2001) Immunisation of cattle with cysteine proteinases of *Trypanosoma congolense*: targetting the disease rather than the parasite. *International Journal of Parasitology* **31**, 1429–1433.

Baral TN (2010) Immunobiology of African trypanosomes: need of alternative interventions. *Journal of Biomedical Biotechnology* **2010**, 389153.

Baral TN, De Baetselier P, Brombacher F and Magez S (2007) Control of *Trypanosoma evansi* infection is IgM mediated and does not require a type I inflammatory response. *The Journal of Infectious Diseases* **195**, 1513–1520.

Barr DB, Landsittel D, Nishioka M, Thomas K, Curwin B, Raymer J, Donnelly KC, McCauley L and Ryan PB (2006) A survey of laboratory and statistical issues related to farmworker exposure studies. *Environmental Health Perspectives* **114**, 961–968.

Bastos IMD, Grellier P, Martins NF, Cadavid-Restrepo G, de Souza-Ault MR, Augustyns K, Teixeira ARL, Schrével J, Maigret B, da Silveira JF and Santana JM (2005) Molecular, functional and structural properties of the prolyl oligopeptidase of *Trypanosoma cruzi* (POP Tc80), which is required for parasite entry into mammalian cells. *Biochemical Journal* **388**, 29–38.

Bastos IMD, Motta FN, Charneau S, Santana JM, Dubost L, Augustyns K and Grellier P (2010) Prolyl oligopeptidase of *Trypanosoma brucei*

hydrolyzes native collagen, peptide hormones and is active in the plasma of infected mice. *Microbes and Infection* **12**, 457–466.

Bastos IMD, Motta FN, Grellier P and Santana JM (2013) Parasite prolyl oligopeptidases and the challenge of designing chemotherapeuticals for Chagas disease, leishmaniasis and African trypanosomiasis. *Current Medicinal Chemistry* **20**, 3103–3115.

Burleigh BA, Caler EV, Webster P and Andrews NW (1997) A cytosolic serine endopeptidase from *Trypanosoma cruzi* is required for the generation of Ca2+ signaling in mammalian cells. *Journal of Cell Biology* **136**, 609–620.

Buxbaum LU (2015) Interleukin-10 from T cells, but not macrophages and granulocytes, is required for chronic disease in *Leishmania mexicana* infection. *Infection and Immunity* **83**, 1366–1371.

Buxbaum LU, Denise H, Coombs GH, Alexander J, Mottram JC and Scott P (2003) Cysteine protease B of *Leishmania mexicana* inhibits host Th1 responses and protective immunity. *The Journal of Immunology* **171**, 3711–3717.

Caffrey CR, Hansell E, Lucas KD, Brinen LS, Alvarez Hernandez A, Cheng J, Gwaltney SL II, Roush WR, Stierhof YD, Bogyo M, Steverding D and McKerrow JH (2001). Active site mapping, biochemical properties and subcellular localization of rhodesain, the major cysteine protease of *Trypanosoma brucei rhodesiense*. *Molecular & Biochemical Parasitology* **118**, 61–73.

Caler EV, Vaena de Avalos S, Haynes PA, Andrews NW and Burleigh BA (1998) Oligopeptidase B-dependent signaling mediates host cell invasion by *Trypanosoma cruzi*. *EMBO Journal* **17**, 4975–4986.

Chomczynski P and Sacchi N (1987) Single-step method of RNA isolation by acid guanidinium thiocyanate-phenol-chloroform extraction. *Analytical Biochemistry* **162**, 156–159.

Claes F, Verloo D, De Waal DT, Urakawa T, Majiwa P, Goddeeris BM and Buscher P (2002) Expression of RoTat 1.2 cross-reactive variable antigen type in *Trypanosoma evansi* and *T. equiperdum*. *Annals of the New York Academy of Sciences* **969**, 174–179.

Coetzer TH, Goldring JP and Huson LE (2008) Oligopeptidase B: a processing peptidase involved in pathogenesis. *Biochimie* **90**, 336–344.

Coustou V, Guegan F, Plazolles N and Baltz T (2010) Complete in vitro life cycle of *Trypanosoma congolense*: development of genetic tools. *PLoS Neglected Tropical Diseases* **4**, e618.

Coustou V, Plazolles N, Guegan F and Baltz T (2012) Sialidases play a key role in infection and anaemia in *Trypanosoma congolense* animal trypanosomiasis. *Cellular Microbiology* **14**, 431–445.

Dargantes AP, Mercado RT, Dobson RJ and Reid SA (2009) Estimating the impact of *Trypanosoma evansi* infection (surra) on buffalo population dynamics in southern Philippines using data from cross-sectional surveys. *International Journal for Parasitology* **39**, 1109–1114.

Desquesnes M, Holzmuller P, Lai DH, Dargantes A, Lun ZR and Jittaplapong S (2013) *Trypanosoma evansi* and surra: a review and perspectives on origin, history, distribution, taxonomy, morphology, hosts, and pathogenic effects. *BioMed Research International* **2013**, 194176.

Fajtová P, Štefanić S, Hradilek M, Dvořák J, Vondrášek J, Jílková A, Ulrychová L, McKerrow JH, Caffrey CR, Mareš M and Horn M (2015) Prolyl oligopeptidase from the blood fluke *Schistosoma mansoni*: from functional analysis to anti-schistosomal inhibitors. *PLoS Neglected Tropical Diseases* **9**, e0003827.

Habila N, Inuwa MH, Aimola IA, Udeh MU and Haruna E (2012) Pathogenic mechanisms of *Trypanosoma evansi* infections. *Research in Veterinary Science* **93**, 13–17.

Herbert WJ and Lumsden WH (1976) *Trypanosoma brucei*: a rapid 'matching' method for estimating the host's parasitemia. *Experimental Parasitology* **40**, 427–431.

Hirumi H and Hirumi K (1989) Continuous cultivation of *Trypanosoma brucei* blood stream forms in a medium containing a low concentration of serum protein without feeder cell layers. *Journal of Parasitology* **75**, 985–989.

Hoare CA (1965) Vampire bats as vectors and hosts of equine and bovine trypanosomes. *Acta Tropica* **22**, 204–216.

Hoare CA (1972) The trypanosomes of mammals. *Journal of Small Animal Practice* **13**, 671–672.

Holland WG, Do TT, Huong NT, Dung NT, Thanh NG, Vercruysse J and Goddeeris BM (2003) The effect of *Trypanosoma evansi* infection on pig performance and vaccination against classical swine fever. *Veterinary Parasitology* **111**, 115–123.

Kangethe RT, Boulange AF, Coustou V, Baltz T and Coetzer TH (2012) *Trypanosoma brucei brucei* oligopeptidase B null mutants display increased prolyl oligopeptidase-like activity. *Molecular & Biochemical Parasitology* **182**, 7–16.

Kaszuba K, Rog T, Danne R, Canning P, Fulop V, Juhasz T, Szeltner Z, St Pierre JF, Garcia-Horsman A, Mannisto PT, Karttunen M, Hokkanen J and Bunker A (2012) Molecular dynamics, crystallography and mutagenesis studies on the substrate gating mechanism of prolyl oligopeptidase. *Biochimie* **94**, 1398–1411.

Kato CD, Alibu VP, Nanteza A, Mugasa CM and Matovu E (2015) Interleukin (IL)-6 and IL-10 are up regulated in late stage *Trypanosoma brucei rhodesiense* sleeping sickness. *PLoS Neglected Tropical Diseases* **9**, e0003835.

Kimura M, Takatsuki A and Yamaguchi I (1994) Blasticidin S deaminase gene from Aspergillus terreus (BSD): a new drug resistance gene for transfection of mammalian cells. *Biochimica et Biophysica Acta (BBA) – Gene Structure and Expression* **1219**, 653–659.

Mbawa ZR, Gumm ID, Shaw E and Lonsdale-Eccles JD (1992) Characterisation of a cysteine protease from bloodstream forms of *Trypanosoma congolense*. *European Journal of Biochemistry* **204**, 371–379.

Medina-Acosta E and Cross GA (1993) Rapid isolation of DNA from trypanosomatid protozoa using a simple 'mini-prep' procedure. *Molecular and Biochemical Parasitology* **59**, 327–329.

Mekata H, Konnai S, Mingala CN, Abes NS, Gutierrez CA, Dargantes AP, Witola WH, Inoue N, Onuma M, Murata S and Ohashi K (2012) Kinetics of regulatory dendritic cells in inflammatory responses during *Trypanosoma evansi* infection. *Parasite Immunology* **34**, 318–329.

Mekata H, Murata S, Mingala CN, Ohashi K and Konnai S (2015) Expression of regulatory dendritic cell-related cytokines in cattle experimentally infected with *Trypanosoma evansi*. *Journal of Veterinary Medical Science* **77**, 1017–1019.

Morty RE, Lonsdale-Eccles JD, Mentele R, Auerswald EA and Coetzer THT (2001) Trypanosome-derived oligopeptidase B is released into the plasma of infected rodents, where it persists and retains full catalytic activity. *Infection and Immunity* **69**, 2757–2761.

Morty RE, Pelle R, Vadasz I, Uzcanga GL, Seeger W and Bubis J (2005) Oligopeptidase B from *Trypanosoma evansi*. A parasite peptidase that inactivates atrial natriuretic factor in the bloodstream of infected hosts. *Journal of Biological Chemistry* **280**, 10925–10937.

Moss CX, Brown E, Hamilton A, Van der Veken P, Augustyns K and Mottram JC (2015) An essential signal peptide peptidase identified in an RNAi screen of serine peptidases of *Trypanosoma brucei*. *PLoS ONE* **10**, e0123241.

Namangala B, De Baetselier P, Noel W, Brys L and Beschin A (2001a) Alternative versus classical macrophage activation during experimental African trypanosomosis. *Journal of Leukocyte Biology* **69**, 387–396.

Namangala B, Noel W, De Baetselier P, Brys L and Beschin A (2001b) Relative contribution of interferon-gamma and interleukin-10 to resistance to murine African trypanosomosis. *Journal of Infectious Diseases* **183**, 1794–1800.

Nyakundi JN, Crawley B and Pentreath VW (2002) The relationships between endotoxins, nitric oxide and inflammatory cytokines in blood and intestinal tissues in experimental *Trypanosoma brucei brucei* infections. *Parasitology* **124**, 597–604.

Patterson HD and Thompson R (1971) Recovery of inter-block information when block sizes are unequal. *Biometrika* **58**, 545–554.

Rawlings ND, Barrett AJ and Finn R (2016) Twenty years of the MEROPS database of proteolytic enzymes, their substrates and inhibitors. *Nucleic Acids Research* **44**, D343–350.

Salah AA, Robertson I and Mohamed A (2015) Estimating the economic impact of *Trypanosoma evansi* infection on production of camel herds in Somaliland. *Tropical Animal Health and Production* **47**, 707–714.

Somanna A, Mundodi V and Gedamu L (2002) Functional analysis of cathepsin B-like cysteine proteases from *Leishmania donovani* complex: evidence for the activation of latent transforming growth factor beta. *Journal of Biological Chemistry* **277**, 25305–25312.

Stijlemans B, Guilliams G, Raes G, Beschin A, Magez S and De Baetselier P (2007) African trypanosomosis: from immune escape and immunopathology to immune intervention. *Veterinary Parasitology* **148**, 3–13.

Sumba AL, Mihok S and Oyieke FA (1998) Mechanical transmission of *Trypanosoma evansi* and *T. congolense* by *Stomoxys niger* and *S. taeniatus* in a laboratory mouse model. *Medical and Veterinary Entomology* **12**, 417–422.

Swenerton RK, Zhang S, Sajid M, Medzihradszky KF, Craik CS, Kelly BL and McKerrow JH (2011) The oligopeptidase B of *Leishmania* regulates parasite enolase and immune evasion. *Journal of Biological Chemistry* **286**, 429–440.

Taylor KA and Authié EM-L (2004) Pathogenesis of animal trypanosomiasis. In Maudlin I, Holmes PH and Miles MA (eds). *The Trypanosomiases*. Wallingford: CABI Publishing, pp. 331–353.

ten Asbroek ALMA, Ouellette M and Borst P (1990) Targeted insertion of the neomycin phosphotransferase gene into the tubulin gene cluster of *Trypanosoma brucei*. *Nature* **348**, 174–175.

Tizard I, Nielsen KH, Seed JR and Hall JE (1978) Biologically active products from African trypanosomes. *Microbiology Reviews* **42**, 664–681.

Vickerman K, Myler PJ and Stuart DK (1993) African trypanosomosis. In Warren KS (ed.). *Immunology and Molecular Biology of Parasitic Infections*. Boston: Blackwell Scientific Publications, pp. 170–212.

Wijewardana V, Kristoff J, Xu C, Ma D, Haret-Richter G, Stock JL, Policicchio BB, Mobley AD, Nusbaum R, Aamer H, Trichel A, Ribeiro RM, Apetrei C and Pandrea I (2013) Kinetics of myeloid dendritic cell trafficking and activation: impact on progressive, nonprogressive and controlled SIV infections. *PLoS Pathogens* **9**, e1003600.

Wirtz E, Leal S, Ochatt C and Cross GA (1999) A tightly regulated inducible expression system for conditional gene knock-outs and dominant-negative genetics in *Trypanosoma brucei*. *Molecular and Biochemical Parasitology* **99**, 89–101.